Research Article

Formulation, Optimization and Characterization of Silver Nanoparticles using *Ardisia crenata* Plant Extract by Green Synthesis Approach: Anticancer Therapeutic Potential

Puja*, Nripendra Singh
Department of Pharmacy, V.B.S. Purvanchal University, Jaunpur-222002, (U.P.) India.
*Corresponding author's E-mail: 24poojasaxena@gmail.com

ABSTRACT

Green synthesis of silver nanoparticles (AgNPs) utilizing plant extracts has gained attention for its eco-friendly and sustainable approach. This study explores the formulation and characterization of AgNPs synthesized using *Ardisia crenata* extract and evaluates their potential therapeutic applications. The plant extract acts as a natural reducing and stabilizing agent, resulting in biocompatible nanoparticles. The synthesis process is optimized using Design Expert software by varying key parameters such as extract concentration, reaction time, and temperature. The formulated AgNPs are characterized through transmission electron microscopy (TEM), Fourier-transform infrared spectroscopy (FTIR) and zeta potential analysis to determine their physicochemical properties. Additionally, in vitro studies, including cytotoxicity assays and apoptosis induction, are conducted to assess their anticancer activity. The findings indicate that these green-synthesized AgNPs exhibit substantial cytotoxic effects on cancer cells, promoting apoptosis and inhibiting proliferation. The initial burst release followed by the prolonged release was observed in optimized formulation. During initial hours minimum burst release of the drug from the *Ardisia crenata* silver nanoparticle was observed followed by prolonged release (68.9%) up to 36h as showed. The study underscores the potential of plant-based AgNPs as promising candidates for biomedical applications, particularly in cancer therapy.

Keywords: *Ardisia crenata*, green synthesis, silver nanoparticles, cytotoxicity.

INTRODUCTION

Cancer remains a major global health concern, driving the need for innovative therapeutic strategies. Nanotechnology, particularly the application of nanoparticles, offers a promising approach to cancer treatment by enabling targeted drug delivery and improving therapeutic outcomes. Among these, silver nanoparticles (AgNPs) have attracted significant interest due to their unique physicochemical properties and potential anticancer effects. However, conventional methods of AgNP synthesis often rely on chemical agents that may pose environmental and health risks, highlighting the need for greener and more biocompatible synthesis approaches [1].

To address these challenges, green synthesis methods using plant extracts have emerged as sustainable and environmentally friendly alternatives for nanoparticle production. *Ardisia crenata*, a medicinal plant rich in bioactive phytochemicals, has shown potential for the green synthesis of AgNPs. Its extract not only acts as a reducing and stabilizing agent for AgNP formation but also imparts additional bioactive compounds that may enhance the nanoparticles' anticancer properties, making it a promising approach for safer and more effective cancer therapy [2].

This study focuses on the formulation and evaluation of silver nanoparticles synthesized using *Ardisia crenata* extract for their potential application in anticancer therapy. By integrating plant-derived bioactive compounds with silver nanoparticles, these nanotherapeutics offer a promising approach to enhancing therapeutic efficacy while addressing the limitations of conventional cancer treatments. Additionally, the adoption of green synthesis methods highlights the significance of sustainability and eco-friendly practices in nanoparticle development [3].

This article aims to explore the challenges in cancer therapy, the role of nanotechnology in overcoming these hurdles, and the rationale for employing green synthesis approaches for AgNP formulation using *Ardisia crenata* extract. Additionally, it examines the potential of *Ardisia crenata*-derived AgNPs as promising anticancer agents, focusing on their formulation techniques, physicochemical properties, and preclinical evaluation. By providing a comprehensive analysis of these aspects, this paper aims to highlight the transformative potential of green-synthesized silver nanoparticles in enhancing cancer treatment strategies [4].

MATERIALS AND METHODS

Ardisia Creneata leaves, roots and fruits were collected from the herbal garden of IFTM University, Moradabad, Uttar Pradesh, India and authenticated from the Department of Botany, IFTM University with reference no. *2020/SOS/BOT/94*. All other solvents and materials used were of analytical grade.

Extract Preparation:

Ardisia crenata extract involves several meticulous steps to ensure the extraction of bioactive compounds with high purity and efficacy. The powdered leaves are then subjected to extraction using a suitable solvent, chosen based on the solubility of the desired compounds, employing techniques such as maceration or Soxhlet extraction. Finally, the concentrated extract is dried again

to eliminate any residual moisture, yielding a crude extract of *Ardisia crenata* ready for storage in sealed containers, safeguarded from light and moisture until further utilization[5].

Preparation of *Ardisia crenata* silver nanoparticle by green synthesis:

A predetermined volume of the *Ardisia crenata* extract is added to a silver nitrate (AgNO3) solution under continuous stirring. The reaction mixture is allowed to incubate at room temperature. The phytochemicals present in the *Ardisia crenata* extract act as reducing and stabilizing agents, facilitating the reduction of silver ions and the formation of silver nanoparticles.

Optimization of Drug Loaded Nanoparticles:

Seventeen sets of experiments were conducted to synthesize silver nanoparticles using *Ardisia crenata* through a green synthesis method, employing the Box Behnken Design to vary formulation variables. A systematic optimization was carried out using the Box–Behnken design of response surface methodology to understand the impact of formulation variables (X1, X2, and X3) on the resulting variables (Y1, Y2, and Y3). This experimental design involved a three-factor, three-level setup, necessitating 17 experiments. Table 1 summarizes the data from these experiments, including independent variables and corresponding responses. Subsequently, the experimental data were used to develop second-order response surface models for Y1, Y2, and Y3, which can be represented by equations 1, 2 and 3 respectively [6].

$$Y_1 = 197 + 5x_1 + 0.40x_2 + 2.15x_3 - 3.15x_1x_2 + 1.28x_1x_3 + 0.24x_2x_3 - 11.6x_1^2 - 2.62x_2^2 - 13.63x_3^2 \quad (1)$$

$$Y_2 = 97.50 + 2.61x_1 + 0.28x_2 + 2.42x_3 - 3.25x_1x_2 - 1.15x_1x_3 + 0.89x_2x_3 - 13.25x_1^2 - 10.38x_2^2 - 5.97x_3^2 \quad (2)$$

$$Y_3 = 78.60 - 1.48x_1 - 0.61x_2 - 0.33x_3 + 1.93x_1x_2 + 4.85x_1x_3 + 1.68x_2x_3 - 4.38x_1^2 - 6.98x_2^2 - 5.89x_3^2 \quad (3)$$

The polynomial equations consist of coefficients representing intercept, first-order main effects, interaction terms, and higher-order effects. These main effects' signs and magnitudes denote the relative influence of each factor on the response, reflecting the average outcome of changing one factor at a time from its lowest to highest value. Interaction terms (X_1X_2, X_1X_3, and X_2X_3) illustrate how the response changes when two factors are simultaneously adjusted. Second-degree terms (X_{12}, X_{22}, and X_{32}) were included to explore non-linearity, where negative signs indicate antagonistic effects and positive signs indicate synergistic effects. Analysis of variance (ANOVA) was utilized to assess the significance of the quadratic second-order models. The surface response models underwent ANOVA analysis at a significance level of 0.0001. In Tables 2 to 4, the results of the ANOVA test on the quadratic regression models are presented. 'Prob>F' values less than 0.05 indicate significant model terms, while 'Lack of Fit' was not significant relative to pure error [7].

Furthermore, model summary statistics revealed R^2 values of 0.9750 for Y^1 (Particle size), 0.9734 for Y_2 (Entrapment efficiency), and 0.9876 for Y_3 (Drug release), indicating a strong correlation between experimental and predicted responses. The predicted R^2 values (0.7865 for Y_1, 0.7165 for Y_2, and 0.9234 for Y_3) were reasonably consistent with the adjusted R^2 values (0.9783 for Y_1, 0.9765 for Y_2, and 0.9768 for Y_3), suggesting model reliability. 'Adequate Precision,' which measures the signal-to-noise ratio, yielded higher values (>4), indicating sufficient signal. The relatively low values of C.V. (coefficient of variation, 1.03 for Y_1, 2.45 for Y_2, and 1.09 for Y_3) suggest better precision and reliability of the experiments conducted [8].

Table 1: Design Matrix and Measured Response for *Ardisia crenata* silver nanoparticles

Run	Factor-A Silver Nitrate	Factor-B Ethanol	Factor-C *Ardisia crenata*	Particle Size (nm)	EE (%)	DR (%)
1	0.05	0.075	0.025	198±3.98	98.5±1.89	77.6±1.23
2	0.04	0.05	0.025	175±7.75	69.8±3.56	68.8±0.42
3	0.06	0.05	0.025	192±3.21	79.8±2.67	62.9±1.89
4	0.04	0.075	0.01	165±5.67	72.8±4.78	73.9±1.98
5	0.06	0.10	0.025	184±4.23	71.5±2.89	65.6±0.25
6	0.06	0.075	0.04	187±2.67	85.5±6.45	68.4±0.37
7	0.05	0.075	0.025	198±7.98	98.5±7.65	77.6±0.39
8	0.05	0.10	0.01	179±9.45	78.8±3.23	61.3±1.20
9	0.05	0.075	0.025	198±2.89	98.5±2.34	77.6±0.12
10	0.05	0.075	0.025	198±8.54	98.5±1.35	77.6±1.65
11	0.05	0.05	0.04	184±9.22	83.8±3.56	62.9±0.25
12	0.05	0.10	0.04	186±6.34	86.5±4.76	66.9±1.90
13	0.05	0.05	0.01	178±8.65	79.6±2.89	67.8±0.35
14	0.04	0.075	0.04	169±6.34	80.8±5.23	62.6±1.89
15	0.06	0.075	0.01	178±8.65	85.9±6.45	60.4±0.25
16	0.05	0.075	0.025	198±4.78	98.5±7.25	77.6±1.57
17	0.04	0.10	0.025	184±3.56	78.5±2.34	63.8±0.67

Data were represented as mean ± SD (n=3).

Table 1 display the results of factor effects and their associated p-values for the responses Y1, Y2, and Y3. The significance of each coefficient was assessed based on the p-value (<0.0001), where smaller p-values indicate greater significance of the corresponding coefficient. The analysis revealed that, at a significant level of $p<0.05$, the significant factors influencing the response Y1 included the synergistic effects of quadratic contributions from X_1, X_1X_3, X_2, and X_3, while the quadratic contribution of X_1X_2 exhibited an antagonistic effect on Y_1. Regarding the response Y_2, significant effects were observed from the synergistic contributions of X_1, X_2, X_3, X_2X_3, as well as the interaction effects of X_1X_2 and X_1X_3. Additionally, the quadratic contribution of interaction effects such as X_1X_2, X_2X_3, and X_1X_3 demonstrated a significant antagonistic effect [9].
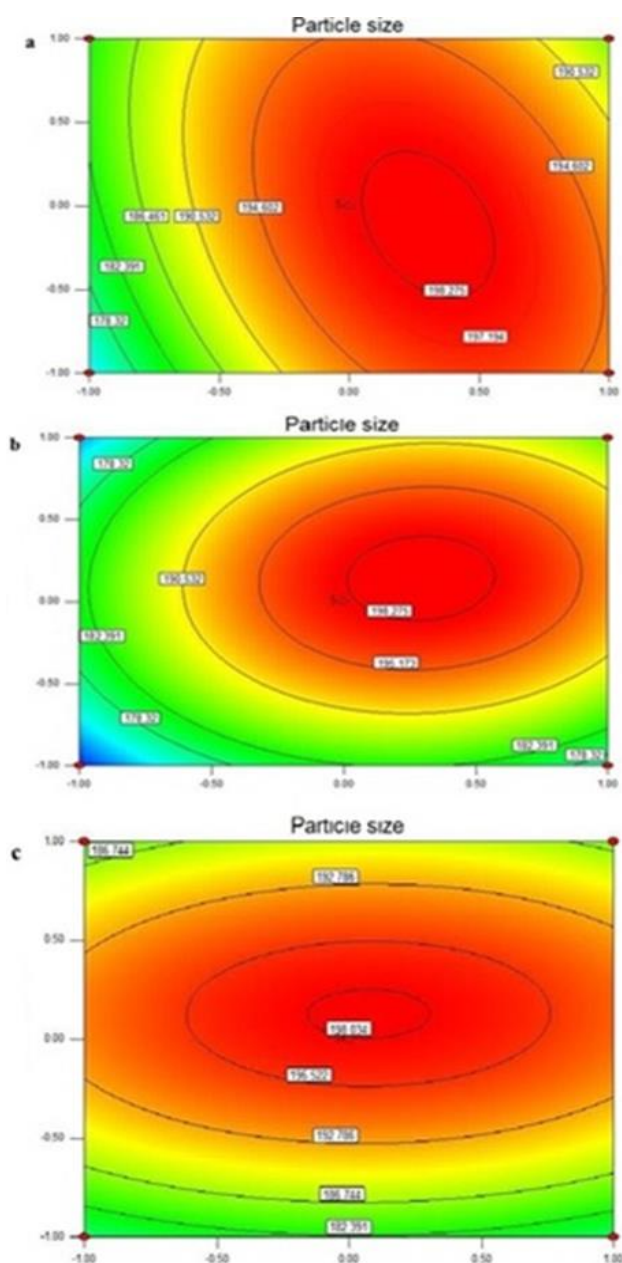

Figure 1: 2 D contour plots showing the effects of the variable on the response. (A) *Ardisia crenata* nanoparticle (B) *Ardisia crenata* silver nanoparticle (C) *Ardisia crenata* silver nanoparticle.

Cytotoxicity and Cell Viability:

MTT Assay (MCF-7 Cell Lines):

The cytotoxicity of the provided samples against the MCF-7 cell line was assessed using the MTT Assay. Initially, cells were seeded at a density of 10,000 cells per well in a 96-well plate and cultured for 24 hours in DMEM medium supplemented with 10% FBS and 1% antibiotic solution at 37°C with 5% CO2. Subsequently, the cells were treated with varying concentrations (ranging from 1 to 1000 μg/ml) of the formulations, which were prepared in incomplete medium. Following a 24-hour incubation period, MTT Solution at a final concentration of 250 μg/ml was added to the cell culture and further incubated for 2 hours. Upon completion of the incubation, the culture supernatant was aspirated, and the cell layer matrix was dissolved in 100 μl Dimethyl Sulfoxide (DMSO). The absorbance was then measured using an Elisa plate reader (iMark, Biorad, USA) at 540 nm and 660 nm wavelengths [10,11,12].

NRU Assay (THP-1 Cell Line):

Cytotoxicity of the provided samples on THP-1 cell line was determined by NRU Assay. The cells (5000-8000 cells/well) were cultured in 96 well plates for 24 h in DMEM medium (AT149- 1L) supplemented with 10% FBS (HIMEDIA-RM 10432) and 1% antibiotic solution at 37°C with 5% CO2. Next day, medium was removed and fresh culture medium was added to each well of the plate. 5 μl of Treatment dilutions (of different concentrations) were added to the defined wells and treated plates were incubated for 24 h. 100 μl of NRU (40 μg/ml in PBS) was added to the defined wells and incubated (Heal Force-Smartcell CO2 Incubator-Hf-90) for 1 h. After that medium was removed, NRU was dissolved in 100 μl of NRU Destain solution. Finally, plates were read at 550/660 nm [13].

MTT Assay (HepG2 cell line):

The cytotoxicity assessment of the provided samples against the HepG2 cell line was conducted using the MTT Assay. Initially, cells were seeded at a density of 10,000 cells per well in a 96-well plate and incubated for 24 hours in DMEM medium supplemented with 10% FBS and 1% antibiotic solution at 37°C with 5% CO2. The following day, cells were exposed to concentrations ranging from 1 to 1000 μg/ml of the formulations, prepared in incomplete medium. Following a 24-hour incubation period, MTT Solution at a final concentration of 250 μg/ml was added to the cell culture and incubated for an additional 2 hours. Upon completion of the incubation, the culture supernatant was aspirated, and the cell layer matrix was dissolved in 100 μl of Dimethyl Sulfoxide (DMSO). Subsequently, the absorbance was measured using an Elisa plate reader at 540 nm and 660 nm wavelengths [14].

Nanoparticle Preparation:

A stock solution of silver nitrate (AgNO₃) was prepared by dissolving a predetermined amount of AgNO₃ in distilled water. Subsequently, the *Ardisia crenata* extract was added to the AgNO₃ solution under continuous stirring at room

temperature. The reaction mixture was then allowed to incubate in the dark for a specific duration, typically ranging from 24 to 48 hours. During this incubation period, the phytochemicals present in the *Ardisia crenata* extract acted as reducing agents, facilitating the reduction of silver ions. This reduction process led to the formation of silver nanoparticles within the reaction mixture. The color change of the reaction mixture, observed over time, served as a visual indicator of the formation of silver nanoparticles, transitioning from yellow to brown, thereby confirming the successful synthesis of silver nanoparticles using the *Ardisia crenata* extract[15].

RESULT AND DISCUSSION

FT- IR of *Ardisia crenata* silver nanoparticle

At 3219.5 cm^-1, the observed O-H stretching vibration signifies the presence of hydroxyl (OH) groups, prevalent in alcohols, phenols, and carboxylic acids. The wave number 2947 cm^-1 corresponds to the C-H stretching vibration characteristic of aliphatic compounds, such as alkanes and alkyl groups, featuring prevalent carbon-hydrogen (C-H) bonds. Observed at 1537 cm^-1, the C=O stretching vibration indicates the presence of the carbonyl (C=O) functional group, commonly encountered in compounds like aldehydes, ketones, carboxylic acids, and esters. The wave number 1267 cm^-1 corresponds to both C-C and C-N stretching vibrations, with C-C stretching typically associated with aromatic rings and C-N stretching characteristic of amines. Finally, at 1074 cm^-1, the observed C-O-C stretching vibration suggests the existence of carbon-oxygen-carbon (C-O-C) bonds, commonly found in ethers, esters, and various organic compounds as shown in figure 2.
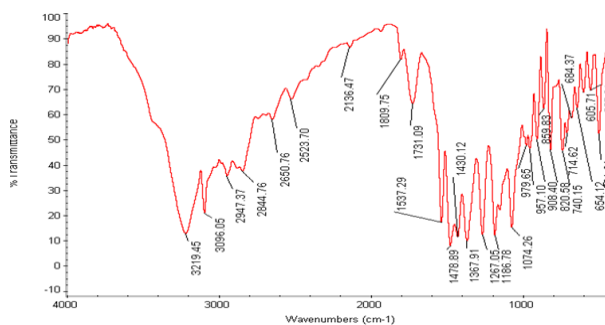

Figure 2: FT-IR Spectrum of *Ardisia crenata* silver nanoparticle

LC-MS ANALYSIS:

The LC-MS analysis was conducted to identify and quantify the compounds present in extract of *Ardisia crenata* and nanoparticle of *Ardisia crenata*. The analysis aimed to characterize the chemical composition of the samples and provide insights into their potential bioactive constituents.

Chromatographic separation was achieved using a C18 column (150 x 2.1 mm, 3.5 µm particle size) with a binary mobile phase consisting of solvent A (acetonitrile) and solvent B (ammonium formate buffer). The MS detector operated in positive ionization mode with a detection wavelength of 280 nm. The retention times and mass spectra of the detected compounds are summarized in Table 2 and figure 3.

Table 2: The retention times and mass spectra of the detected compounds

| R. Time	Score	Compound Name	Ion	Formula	Exact Mass	Observed Mass	Mass Diff
1.28	0.843	Safranine	Positive	C20H19N4	315.16	315.4673	-0.3073
1.55	0.852	Petunidin	Positive	C16H13O7	317.066	315.4673	1.5987
1.59	0.837	Isorhamnetin	[M+H]+	C16H12O7	316.28	315.4673	0.8127
1.72	0.773	Isorhamnetin	[M+H]+	C16H12O7	316.28	315.4673	0.8127
15.27	0.892	Luteolin	Positive	C15H10O6	286.047	285.4967	0.5503
15.37	0.914	Luteolin	Positive	C15H10O6	286.047	285.4227	0.6243
16.91	0.972	Methyl Jasmonate	Positive	C13H20O3	224.141	224.6305	-0.4895
17.08	0.981	L-Carnosine	[M+H]+	C9H14N4O3	226.23	224.5565	1.6735
17.15	0.951	Methyl Jasmonate	Positive	C13H20O3	224.141	224.5935	-0.4525
17.28	0.989	Flavanone	Positive	C15H12O2	224.083	224.5195	-0.4365
17.45	0.935	Methyl Jasmonate	Positive	C13H20O3	224.141	224.5935	-0.4525
17.83	0.914	DL-Dihydrozeatin	Positive	C10H15N5O	221.127	224.5935	-3.4665
17.93	0.895	Flavanone	Positive	C15H12O2	224.083	224.4825	-0.3995
23.56	0.639	Adenosine-3',5'-cyclicmonophosphate	[M+H]+	C10H12N5O6P	329.21	329.6016	-0.3916
23.66	0.66	Malvidin Chloride	Positive	C17H15O7	331.081	329.6016	1.4794
23.83	0.717	Scoulerin	Positive	C19H21NO4	327.147	329.5646	-2.4176
23.90	0.659	Adenosine-3',5'-cyclicmonophosphate	Positive	C10H12N5O6P	329.052	329.6016	-0.5496
24.00	0.61	Adenosine-3',5'-cyclicmonophosphate	Positive	C10H12N5O6P	329.052	329.6386	-0.5866
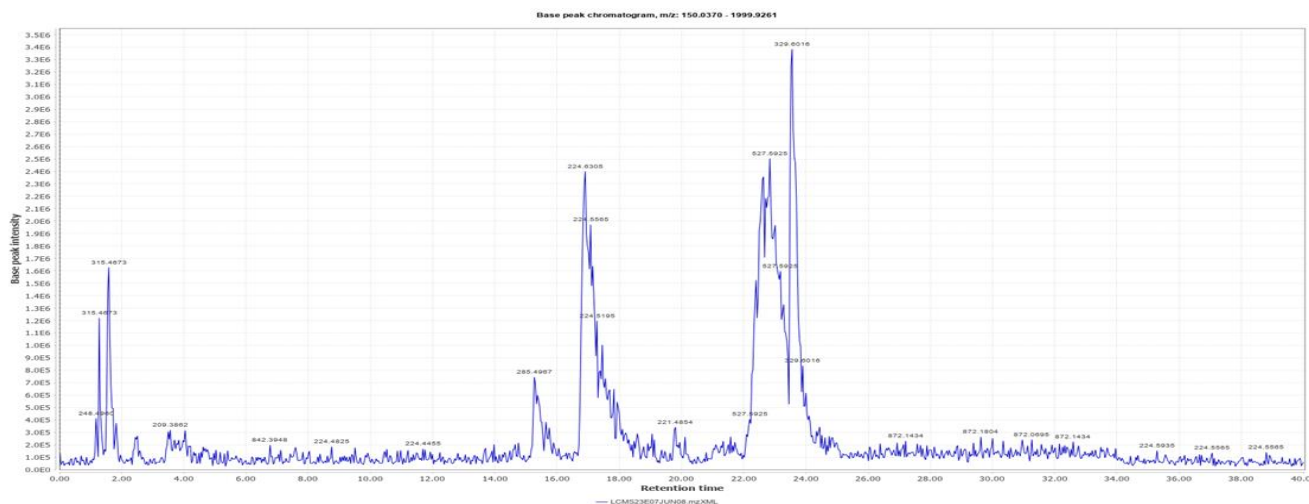
Figure 3: LC-MS spectra of *Ardisia crenata* plant extract

Cytotoxicity and Cell Viability:

MTT Assay (MCF-7 Cell Lines):

The IC$_{50}$ value of *Ardisia crenata* for the MCF-7 cell line is 753.4 µg/ml. This IC$_{50}$ value represents the concentration of *Ardisia crenata* required to inhibit the growth of MCF-7 cancer cells by 50% in vitro. A higher IC$_{50}$ value indicates that a larger concentration of the sample is needed to achieve 50% inhibition of cell proliferation. In this case, the relatively high IC$_{50}$ value of 753.4 µg/ml for *Ardisia crenata* suggests that a significant concentration of the compound is necessary to exert cytotoxic effects against MCF-7 cells. It's important to note that while *Ardisia crenata* may exhibit cytotoxicity against MCF-7 cells at higher concentrations[17,18,19].

NRU Assay (THP-1 Cell Line):

The IC$_{50}$ value of ACP-1124 for the THP-1 cell line is 15.06 µg/ml. This IC$_{50}$ value represents the concentration of *Ardisia crenata* required to inhibit cell viability by 50% in vitro, as assessed by the Neutral Red Uptake (NRU) assay. A lower IC$_{50}$ value indicates that a smaller concentration of the sample is needed to induce cytotoxic effects, leading to a 50% reduction in cell viability. In this case, the relatively low IC$_{50}$ value of 15.06 µg/ml for *Ardisia crenata* suggests that the compound exhibits significant cytotoxicity against THP-1 cells at relatively low concentrations. The result implies that *Ardisia crenata* has potential as a cytotoxic agent against THP-1 cells in vitro[20].

MTT Assay (HepG2 cell line):

The IC$_{50}$ value of *Ardisia crenata* for the HepG2 cell line is 324.8 µg/ml. This IC$_{50}$ value represents the concentration of *Ardisia crenata* required to inhibit cell viability by 50% in vitro, as determined by the assay performed using HepG2 cells. The IC50 value is an important indicator of the compound's potency in exerting cytotoxic effects on the tested cells. In this case, the relatively high IC$_{50}$ value of 324.8 µg/ml suggests that a considerable concentration of *Ardisia crenata* is needed to achieve a 50% reduction in cell viability in HepG2 cells.[21].

CHARACTERIZATION OF OPTIMIZED *ARDISIA CRENATA* SILVER NANOPARTICLE

Measurement of Particle size

The nanoparticle size is affected by the varying concentrations of the polymeric system and drug. The size of the optimized formulation was 659.8 nm with the poly dispersity index of 0.349 showed in Figure 4. The zeta potential of the optimized formulation was –11.9 mV showed in Figure 5.
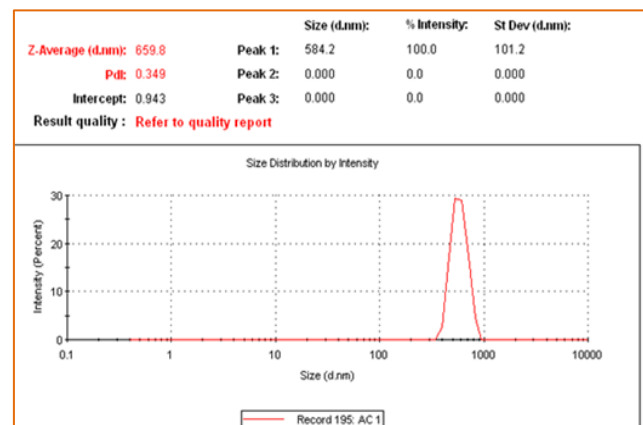

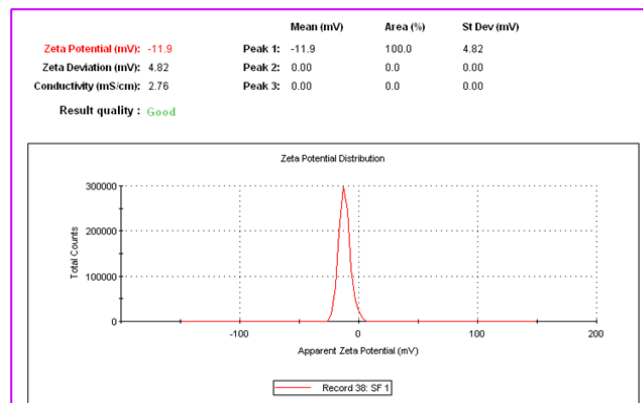**Figure 4:** Particle size of *Ardisia crenata* Silver Nanoparticle

Figure 5: Zeta Potential (mV) of *Ardisia crenata* silver nanoparticle

TEM Analysis

TEM image analysis corroborated that particles with narrow size distributions were successfully synthesized through a counter ion induced gellification method. As depicted in Figure 4, the particles exhibited nanometer-scale spherical shapes, with sizes ranging around 200 nm for the silver nanoparticles derived from *Ardisia crenata* the formation of smoother and more spherical particles, as illustrated in Figure 6.
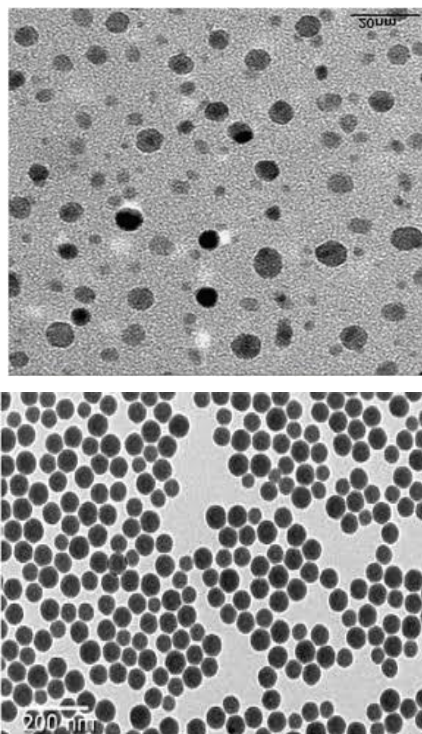

Figure 6: TEM image of *Ardisia crenata* silver nanoparticle

Entrapment efficiency and Drug loading

The entrapment efficiency of a formulation is influenced by various factors, including the concentrations of polymers and drug components. Therefore, a systematic optimization process was conducted to determine the optimal concentrations. Following optimization, the entrapment efficiency of the formulated system reached a high value of 93.59%. Additionally, the percentage of drug loading in the formulation was determined to be 39.80%.

In Vitro Drug Release

The dialysis bag method has been frequently reported for this purpose as it facilitates the separation of the released drug from the bound drug. However, the release rate of the drug is usually affected by the diffusional resistance of the membrane [22,24,25].

The percentage release of free drug *Ardisia crenata* was somewhat greater when compared to that of *Ardisia crenata* silver nanoparticles. The percentage of *Ardisia crenata* released from the nanoparticles initially rapid and then very slow after some which was consistent with the phenomena reported by the authors [23,26,27].

The initial burst release followed by the prolonged release

was observed in optimized formulation. During initial hours minimum burst release of the drug from the *Ardisia crenata* silver nanoparticle was observed followed by prolonged release (68.9%) up to 36h as showed in Figure 7. Prolonged release was obtained due to electrostatic interaction of composites, leading to slow diffusion of the drug from the polymeric matrix. Due to the increased diffusional distance and hindering effects by the surrounding polymeric network, the drug has a controlled release profile.
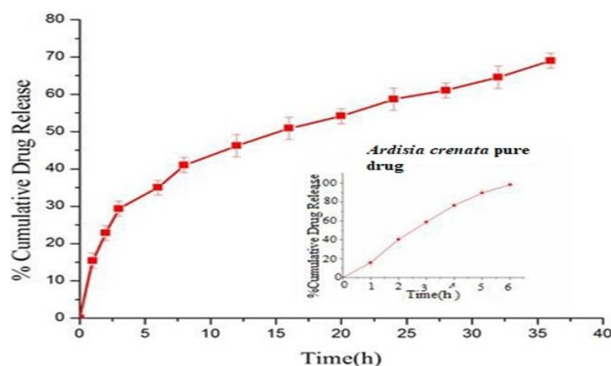

Figure 7: *In vitro* drug release profile of *Ardisia crenata* from polymeric nanoparticles and free drug

CONCLUSION

Studies of *Ardisia crenata* extract have various bioactive compounds, it shows strong antioxidant properties and protecting cells against various types of cancer. These extracts reduce free radicals' level and preventing cancer initiation and progression. Studies for the MCF-7 cell line, *Ardisia crenata* exhibited an IC50 value of 753.4 µg/ml, indicating relatively weak cytotoxicity against cancer cells. However, in the THP-1 cell line, the IC50 value was significantly lower at 15.06 µg/ml, suggesting potent cytotoxic effects against leukemia cells. Moreover, when tested on the HepG2 cell line, *Ardisia crenata* showed an IC50 value of 324.8 µg/ml, indicating moderate cytotoxicity against cancer cells. The findings by MTT assay confirm the anticancer potentials of *Ardisia crenata* extract and leukemia cells exhibiting the highest sensitivity to the extracts. The observed cytotoxic effects of *Ardisia crenata* extracts against cancer cell lines highlight the clinical relevance as potential candidate for further studies in cancer treatment and reducing various side effects of chemotherapy and radiotherapy. The initial burst release followed by the prolonged release was observed in optimized formulation. During initial hours minimum burst release of the drug from the *Ardisia crenata* silver nanoparticle was observed followed by prolonged release up to 36h as showed. Overall, these results provide a foundation for future research on the cytotoxic potential of *Ardisia crenata* and their impacts on human health for the development of novel, natural and most effective therapeutic agents in form of dosage forms.

Conflict of Interest: The author(s) declared no potential conflicts of interest with respect to the research, authorship, and/or publication of this article.

REFERENCES

1. Bhattacharya R, Mukherjee P. Biological properties of "naked" metal nanoparticles. Adv Drug Deliv Rev. 2008; 60(11):1289-1306.

2. Kim SM, Lee SH, Ryu DS, Choi SJ, Lee DS. Green synthesis of silver nanoparticles using *Ardisia crenata* extract for antibacterial and catalytic activities. Mater Lett. 2019; 246:18-21.

3. Khatami M, Varma RS, Zafarian S, Rahdar A, Cupakova S, Hajivalili M, et al. Green biosynthesis of silver nanoparticles using *Quercus brantii* (oak) leaves hydroalcoholic extract and their antibacterial activity. Mater Sci Eng C. 2016; 63:282-287.

4. Sharma N, Ojha H, Bharadwaj A, Pathak DP, Sharma RK. Green synthesis of metallic nanoparticles as effective alternatives to overcome multidrug resistance in cancer chemotherapy: A review. Int J Pharm. 2021; 601:120561.

5. Kim SM, Lee SH, Ryu DS, Choi SJ, Lee DS. Green synthesis of silver nanoparticles using *Ardisia crenata* extract for antibacterial and catalytic activities. Mater Lett. 2019; 246:18-21.

6. Gholibegloo E, Karimi M, Jalili-Baleh L, Shirbandi K, Amjad K, Hadizadeh F. Design of experiments (DoE) optimization of capsaicin-loaded solid lipid nanoparticles for enhanced anti-angiogenic cancer therapy. RSC Adv. 2020; 10(24):14206-14217.

7. Nawaz H, Gull N, Zafar B, Jabeen N, Qasim M, Nazar M, Nazir A. Design of experiment optimization for green synthesis of silver nanoparticles loaded with plant extracts: Anticancer and antimicrobial study. Arab J Chem. 2020;13(1):2896-2908.

8. Ahmad N, Sharma S, Singh VN, Shamsi SF, Fatma A. Measuring the effect of cadmium and selenium exposure on nanoparticle-treated cancer cells using a 3D model of tumor-macrophage interaction. Sci Rep. 2015; 5:15607.

9. Jena P, Mohanty S, Mallick R, Jacob B, Sonawane A. Toxicity and antibacterial assessment of chitosan-coated silver nanoparticles on human pathogens and macrophage cells. Int J Nanomedicine. 2013;8:1497-1518.

10. Blois MS. Antioxidant determinations by the use of a stable free radical. Nature. 1958;181(4617):1199-1200.

11. Re R, Pellegrini N, Proteggente A, Pannala A, Yang M, Rice-Evans C. Antioxidant activity applying an improved ABTS radical cation decolorization assay. Free Radic Biol Med. 1999;26(9-10):1231-1237.

12. Mosmann T. Rapid colorimetric assay for cellular growth and survival: Application to proliferation and cytotoxicity assays. J Immunol Methods. 1983;65(1-2):55-63.

13. Borenfreund E, Babich H, Martin-Alguacil N. Comparisons of two in vitro cytotoxicity assays: The neutral red (NR) and tetrazolium MTT tests. Toxicol In Vitro. 1988;2(1):1-6.

14. Denizot F, Lang R. Rapid colorimetric assay for cell growth and survival: Modifications to the tetrazolium dye procedure giving improved sensitivity and reliability. J Immunol Methods. 1986;89(2):271-277.

15. Singh P, Kim YJ, Zhang D, Yang DC. Biological synthesis of nanoparticles from plants and microorganisms. Trends Biotechnol. 2016;34(7):588-599.

16. Yang L, Hu J, Shen Z, Chen Y, Chen J, Luo H. X-ray diffraction analysis of polymeric nanoparticles. J Nanosci Nanotechnol. 2020;20(10):6552-6557.

17. Sanches-Silva A, Cruz R, Costa D, Albuquerque TG. Antioxidant capacity of plant foods: Assessment methods and recent trends. Food Rev Int. 2018;34(2):170-196.

18. Re R, Pellegrini N, Proteggente A, Pannala A, Yang M, Rice-Evans C. Antioxidant activity applying an improved ABTS radical cation decolorization assay. Free Radic Biol Med. 1999;26(9-10):1231-1237.

19. Mosmann T. Rapid colorimetric assay for cellular growth and survival: Application to proliferation and cytotoxicity assays. J Immunol Methods. 1983;65(1-2):55-63.

20. Borenfreund E, Puerner JA. A simple quantitative procedure using monolayer cultures for cytotoxicity assays (HTD/NR-90). J Tissue Cult Methods. 1984;9(1):7-9.

21. Mosmann T. Rapid colorimetric assay for cellular growth and survival: Application to proliferation and cytotoxicity assays. J Immunol Methods. 1983;65(1-2):55-63.

22. Costa P, Sousa Lobo JM. Modeling and comparison of dissolution profiles. Eur J Pharm Sci. 2001;13(2):123-133.

23. Liu C, Gong Z, Yang S, Zheng X, Lu W, Zhang Y. Release behavior and mechanism of *Ardisia crenata* extract from liposomes in vitro. Drug Dev Ind Pharm. 2017;43(9):1550-1557.

24. Saxena P., Singh N., and Singh SK. *Ardisia crenata*: A New Source of Health Promoting Phytopharmaceuticals and Chemicals. *Journal of Pharmaceutical Negative Results*, 2022;13(10): 4907-4914. https://doi.org/10.47750/pnr.2022.13.S10.595.

25. Singh SK., Singh N., and Saxena P. Therapeutic Nanoparticles: A Promising Drug Delivery System. *Journal of Pharmaceutical Negative Results*, 2022, 13(10): 4915-4927. https://doi.org/10.47750/pnr.2022.13.S10.596.

26. Singh Y, Koshy MK, Saraf SA, Singh N. Gelatin Adsorbed Solid Lipid Nanoparticles (SLN) for Targeted Drug Delivery of Anti-Inflammatory Drug. *Journal of Pharmaceutical Negative Results*, 2022;13(05): 2845 2853. https://doi.org/10.47750/pnr.2022.13.S05.431.

27. Singh N, Singh R. An Introduction to the Approaches of Novel Drug Delivery Systems for Acquired Immune Deficiency Syndrome (AIDS). Journal of AIDS and HIV Infections, 2016;2(1): 103-09. Doi: 10.15744/2454-499X.2.103.

For any questions related to this article, please reach us at: globalresearchonline@rediffmail.com

New manuscripts for publication can be submitted at: submit@globalresearchonline.net and submit_ijpsrr@rediffmail.com